Development 133, 3587-3595 (2006) doi:10.1242/dev.02539

Mesodermal expression of *Tbx1* is necessary and sufficient for pharyngeal arch and cardiac outflow tract development

Zhen Zhang[1,2,*], Tuong Huynh[2,*] and Antonio Baldini[1,2,3,*,†]

The development of the segmented pharyngeal apparatus involves complex interaction of tissues derived from all three germ layers. The role of mesoderm is the least studied, perhaps because of its apparent lack of anatomical boundaries and positionally restricted gene expression. Here, we report that the mesoderm-specific deletion of *Tbx1*, a T-box transcription factor, caused severe pharyngeal patterning and cardiovascular defects, while mesoderm-specific restoration of *Tbx1* expression in a mutant background corrected most of those defects in the mouse. We show that some organs, e.g. the thymus, require *Tbx1* expression in the mesoderm and in the epithelia. In addition, these experiments revealed that different pharyngeal arches require *Tbx1* in different tissues. Finally, we show that *Tbx1* in the mesoderm is required to sustain cell proliferation. Thus, the mesodermal transcription program is not only crucial for cardiovascular development, but is also key in the development and patterning of pharyngeal endoderm.

KEY WORDS: *Tbx1*, *Fgf8*, DiGeorge syndrome, 22q11DS, Mesoderm, Anterior heart field, Pharyngeal development, Cardiac outflow tract, Thymus, Mouse

INTRODUCTION

The pharyngeal apparatus is an important transient embryonic structure composed of a series of reiterated bulges, called pharyngeal arches, that give rise to a variety of craniofacial, cervical and thoracic organs and structures. Perturbation of normal pharyngeal development causes many congenital diseases, such as DiGeorge syndrome (reviewed by Lindsay, 2001) and branchio-oto-renal syndrome (Chen et al., 1995), Opitz syndrome (Robin et al., 1995). Pharyngeal morphogenesis requires precisely co-coordinated interaction of pharyngeal endoderm, surface ectoderm, pharyngeal and splanchnic mesoderm, and neural crest-derived cells. Classic avian embryonic transplantation studies (Noden, 1983) suggest that the neural crest may play a primary role in patterning the pharyngeal apparatus. However, Trainor et al. have suggested that the maintenance of transplanted neural crest cell fate in those experiments might be due to co-transplanted isthmic tissue (Trainor et al., 2002a). Other studies suggest that neural crest cells need environmental signals to maintain their identity (Saldivar et al., 1996; Trainor and Krumlauf, 2000). In addition, it has been shown that pharyngeal arch segmentation and the formation of the 2nd and 3rd pharyngeal pouches can occur in the absence of neural crest cells in chick (Veitch et al., 1999). Although these data do not support a primary role of neural crest cells in patterning the pharyngeal arches, other studies have shown that these cells have an instructive role in patterning facial structures (Helms and Schneider, 2003; Schneider and Helms, 2003). More recently, it has been suggested that pharyngeal endoderm may play an important role in pharyngeal patterning (Graham et al., 2005). For example, the zebrafish *Tbx1* mutant *vgo* exhibited severe segmentation defects that could be partially corrected by transplantation of wild-type endoderm-fated cells (Piotrowski et al., 2003; Piotrowski and Nusslein-Volhard, 2000). However, whether or not the pharyngeal mesoderm has a role in pharyngeal segmentation is unclear.

Tbx1 encodes a transcription factor of the T-box gene family. The gene is haploinsufficient in humans, and is thought to play a major role in the pathogenesis of DiGeorge syndrome (Jerome and Papaioannou, 2001; Lindsay et al., 2001; Merscher et al., 2001; Yagi et al., 2003). Investigators have accumulated a substantial amount of data supporting interactions between Tbx1 and major signaling systems such as the fibroblast growth factor (FGF) (Hu et al., 2004; Vitelli et al., 2002b; Xu et al., 2004), hedgehog (Yamagishi et al., 2003), retinoic acid (Guris et al., 2006; Roberts et al., 2005) and vascular endothelial growth factor (Stalmans et al., 2003) signaling. These reports underscore the intricacy of the role of Tbx1 in mammalian embryonic development. We and others have initiated an extensive dissection of the mouse mutant phenotype using conditional time- and tissue-specific ablation and dose manipulation (Arnold et al., 2006; Hu et al., 2004; Liao et al., 2004; Xu et al., 2005; Xu et al., 2004; Zhang et al., 2005). Results indicated that at all developmental times and in most tissues tested there is a crucial role for *Tbx1*, and that different structures have different sensitivity to *Tbx1* dose.

Tbx1 is mainly expressed in tissues that form the embryonic pharyngeal system, i.e. surface ectoderm, pharyngeal endoderm, head mesenchyme, core mesoderm, splanchnic mesoderm, but not neural crest-derived mesenchyme (Chapman et al., 1996; Vitelli et al., 2002a). The pharyngeal endoderm expression domain has stimulated considerable attention because of its dynamic nature, and because mutants have hypoplasia and defective segmentation of the pharynx (Jerome and Papaioannou, 2001; Lindsay et al., 2001; Vitelli et al., 2002a). Indeed, *Tbx1* ablation reduces the proliferation of endodermal cells (Xu et al., 2005), while heterozygous ablation of the gene in pharyngeal epithelia (ectoderm and endoderm but not in the mesoderm) causes vascular abnormalities characteristic of the *Tbx1* haploinsufficiency phenotype (Zhang et al., 2005). In addition, it has been shown that

[1]Program in Cardiovascular Sciences, Baylor College of Medicine, Houston, TX 77030, USA. [2]Department of Pediatrics (Cardiology), Baylor College of Medicine, Houston, TX 77030, USA. [3]Department of Molecular and Human Genetics, Baylor College of Medicine, Houston, TX 77030, USA.

*Present address: Alkek Institute of Biosciences and Technology, Texas A&M System Health Science Center, 2121 W. Holcombe Blvd. room 820c, Houston, TX 77030, USA

[†]Author for correspondence (e-mail: abaldini@ibt.tamhsc.edu)

Accepted 18 July 2006

homozygous, conditional ablation of *Tbx1* by the *Foxg1*^{Cre} driver, which induces recombination predominantly in the pharyngeal endoderm, causes a mutant phenotype similar to that of germ line null mutants. However, tissues that express *Tbx1* interact closely during development, raising the issue of whether *Tbx1* may be required in multiple tissues to contribute to morphogenesis of the pharyngeal system. In this study, we use a novel approach, i.e. tissue-specific re-activation of the gene in a mutant background, as well as classic tissue-specific gene ablation, to address this. Results show that most of the developmental defects generated by null mutation of *Tbx1* are recapitulated by mesodermal-specific somatic deletion of the gene, while mesodermal reactivation of the gene in a mutant background rescues most of those defects. Our data revealed a previously unknown instructive role of mesoderm in patterning pharyngeal segmentation. In addition, the combination of tissue-specific ablation and tissue-specific re-activation revealed different requirements of *Tbx1* expression in the development of different pharyngeal structures. Our in vivo analysis suggests that mesodermal *Tbx1* expression supports proliferation and regulates the expression of *Fgf8* in the splanchnic mesoderm/anterior heart field.

MATERIALS AND METHODS

Mouse mutants and breeding

All the experiments involving mice were approved by the Institutional Animal Care and Use Committee of Baylor College of Medicine, and in compliance with the USA Public Health Service Policy on Humane Care and Use of Laboratory Animals.

The following mouse mutant alleles used in this study have been reported previously: *Tbx1*^{flox}, *Tbx1*$^{\Delta E5}$, *Tbx1*^{mcm} (Xu et al., 2004), *Tbx1*^{lacZ} (Lindsay et al., 2001), *Mesp1*^{Cre} (Saga et al., 1999) and R26R (Soriano, 1999). All lines were backcrossed into the C57Bl/6 genetic background for at least two generations. PCR strategies for mouse genotyping have been described in the original reports.

The *Tbx1*^{neo2} allele was generated by gene targeting in AB2.2 ES cells, as shown in Fig. 3A. A loxP-flanked PGKneo cassette (neomycin resistant gene driven by the PGK promoter) was inserted in an intron between exon 5 and exon 6 of *Tbx1* by homologous recombination. ES cells were injected into C57BL/6 blastocysts and chimeric mice were crossed with C57BL/6 mice to obtain germ line transmission of the mutant allele. The *Tbx1*^{neo2} allele was genotyped with primer pair 5′-GCCAGAGGCCACTTGTGTAG-3′ and 5′-AGGCTGGGATTCCAAAAGAC-3′.

Quantification of *Tbx1* expression level

Quantification of *Tbx1* expression was carried out using the TaqMan Gene Expression Assay system (Applied Biosystem) on total RNA extracted from E9.5 wild-type, *Tbx1*$^{neo2/+}$, *Tbx1*$^{neo2/neo2}$ and *Tbx1*$^{neo2/-}$ embryos. We used commercially available probe and primer sets (assay IDs are Mm01342800_gH for *Tbx1* and Mm00607939_s1 for the β-actin control).

Tamoxifen-induced Cre recombination

We used an inducible allele *Tbx1*$^{mcm/+}$ to map the distribution of *Tbx1*-expressing cells during embryogenesis as previously described (Xu et al., 2005). We injected tamoxifen (Sigma) intraperitoneally into pregnant female (75 mg/kg body weight) at E6.5 and half this dose on the following 2 days.

Morphological analysis

Aortic arch arteries and hearts of E18.5 embryos were isolated by manual dissection and photographed under a stereomicroscope. Hearts were embedded, sectioned and stained with Hematoxylin and Eosin. Earlier embryos were examined under the stereomicroscope, fixed and embedded in paraffin for histological analysis. Intracardiac ink injection was performed to visualize pharyngeal arch arteries at E10.5. Embryos were then fixed and dehydrated in ethanol:water:acetic acid:chloroform (95:3:1:1) solution and cleared in methyl salicylate:benzyl benzoate (50:50) solution. β-Galactosidase activity was revealed by staining paraformaldehyde-fixed embryos with the X-gal substrate, according to standard procedures. Stained whole-mount embryos were photographed and then embedded in paraffin and cut into 10 μm histological sections. Sections were counterstained with Nuclear Fast Red.

RNA in situ hybridization and immunohistochemistry

Whole-mount and tissue section RNA in situ hybridization with non-radioactive probes was performed as previously described (Albrecht et al., 1997), using probes for *Pax1* (kindly provided by Dr R. Balling), *Tbx1* (from Dr V. Papaioannou), *Crabp1* (Giguere et al., 1990) and *Fgf8* (from Dr G. Martin). The anti Hoxb1 antibody has been kindly provided by Dr N. Manley. The anti neurofilament-M monoclonal antibody 2H3 was obtained from the Developmental Studies Hybridoma Bank. Anti Hoxb1 and neurofilament-M were used in whole-mount immunohistochemistry. Proliferating cells were labeled by immunohistochemistry on paraffin-embedded sections using an anti phosphorylated histone H3 antibody (Upstate) and assayed on three controls and three conditional mutants. Tissue-specific deletion and restoration of *Tbx1* expression was confirmed by immunofluorescence on cryosections with an anti Tbx1 antibody (Zymed).

RESULTS

Mesp1^{Cre} induces deletion of a conditional *Tbx1* allele in the mesoderm but not in the endoderm

Mesp1 is initially expressed in epiblast cells sorting through the primitive streak and is quickly downregulated after E7 (Saga et al., 1999), i.e. before *Tbx1* is turned on. The progeny of *Mesp1*-expessing cells contributes heavily to the cranial mesoderm (Saga et al., 1999; Zhang et al., 2005). *Mesp1*^{Cre}-induced recombination, as visualized by crosses with the R26R reporter (Soriano, 1999), is restricted to mesodermally derived tissues and was not detected in endodermal or ectodermal cells (Fig. 1B). Based on fate mapping of *MespI*-expressing and *Tbx1*-expressing cells (Fig. 1A), we expected that *Mesp1*^{Cre} would ablate *Tbx1* expression in all its mesodermal domains of the pharynx, head mesenchyme and splanchnic mesoderm. To conditionally ablate *Tbx1* in these domains, we crossed *Mesp1*$^{cre/+}$;*Tbx1*$^{\Delta E5/+}$ mice with *Tbx1*$^{flox/flox}$ mice. Immunohistochemistry using an anti Tbx1 antibody confirmed the loss of the protein in mesodermally derived tissues but not in the endoderm of *Mesp1*$^{cre/+}$;*Tbx1*$^{\Delta E5/flox}$ embryos at E9.5 (Fig. 1C,D), although we did detect some residual Tbx1 immunoreactivity in the core of the 1st pharyngeal arch (arrow in Fig. 1D). At E9.0, we obtained a similar result and confirmed the preservation of the ectodermal signal (Fig. 1E-F). Thus, *Mesp1*^{Cre}-driven deletion is specific for the mesoderm and does not affect (directly or indirectly) epithelial expression of *Tbx1*.

Mesodermal deletion of *Tbx1* causes severe phenotypic abnormalities

We examined the morphological phenotype of *Mesp1*$^{cre/+}$;*Tbx1*$^{\Delta E5/flox}$ embryos (hereafter referred to as M-ko) at different developmental stages. At E18.5, M-ko embryos (n=15) exhibited a phenotype very similar to that observed in *Tbx1*$^{-/-}$ embryos. In particular, M-ko embryos had hypoplastic external ears (15/15, Fig. 2A,A′), thymic aplasia or severe hypoplasia (12/15 and 3/15, respectively, Fig. 2B,B′), persistent truncus arteriosus (PTA) and ventricular septal defects (VSD) (15/15, Fig. 2C-D′), as well as aortic arch defects (15/15, Fig. 2C,C′). However, with one exception, M-ko embryos did not exhibit cleft palate, a common feature of *Tbx1*$^{-/-}$ mutants (not shown). At E10.5, M-ko embryos (n=15) presented with hypoplasia of the 2nd pharyngeal arches (Fig. 2E,E′), loss of the 3rd, 4th and 6th pharyngeal arches and pharyngeal arch arteries (PAA) (Fig. 2F,F′), and severe hypoplasia of the pharynx (Fig. 2G,G′). RNA in situ hybridization with *Pax1*, a marker of pharyngeal pouch endoderm, showed no labeling of the

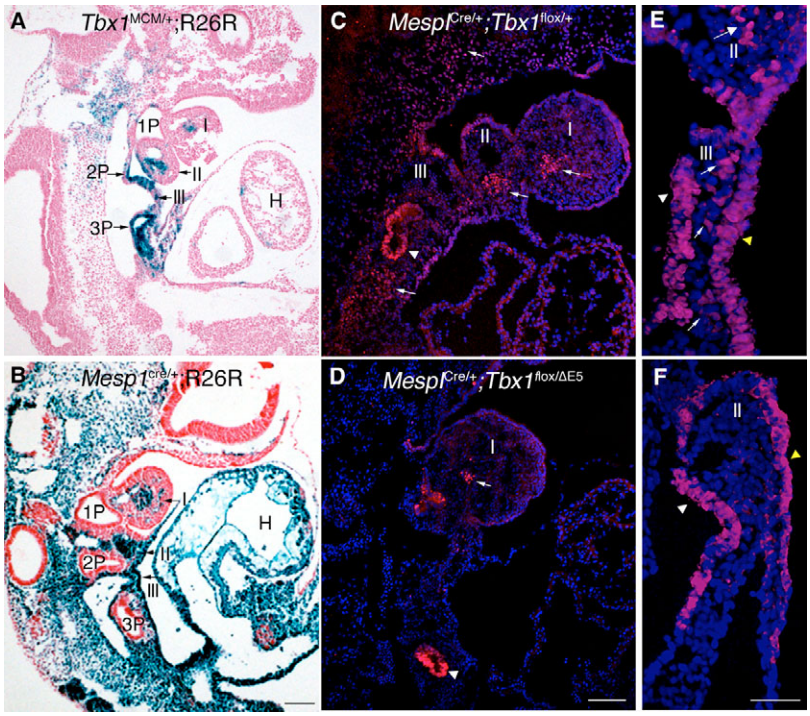

Fig. 1. Mesodermal-specific deletion of *Tbx1* by *Mesp1*^{Cre}. (**A-D**) Sagittal sections of E9.5 embryos. (A) Distribution of *Tbx1*-traced cells visualized by crossing *Tbx1*$^{mcm/+}$ mice with the reporter R26R, compared with the distribution of *Mesp1*^{Cre}-traced cells (B). Recombination is absent in the endoderm in the latter experiment. (C,D) Immunofluorescent staining with an anti-Tbx1 antibody on control (C) and conditional mutant (D) E9.5 embryos. Tbx1 immunoreactivity is preserved in the endoderm (arrowheads) and, to a lesser extent, in the core of the 1st pharyngeal arch (arrow in D), but not in other mesodermal domains (arrows). (**E**,**F**) Coronal sections of E9 embryos. Immunofluorescent staining with an anti-Tbx1 antibody on control (E) and M-ko embryos (F). Mesodermal expression (arrows) is eliminated in M-ko embryos, but endodermal (white arrowhead) and ectodermal (yellow arrowhead) expression are maintained. I, II and III, 1st, 2nd and 3rd pharyngeal arches; 1P, 2P and 3P, 1st, 2nd and 3rd pharyngeal pouches. Scale bar: 100 μm in A-D; 50 μm in E,F.

2nd and 3rd pharyngeal pouches of M-ko embryos (Fig. 2J,J′), while the 4th pouch, identified by immunohistochemistry with an anti Hoxb1 antibody, appeared to be smaller (Fig. 2K,K′) though not as severely affected as that of null mutants (data not shown). These data suggest that Tbx1 in the mesoderm regulates a signaling pathway required for pharyngeal endoderm development.

Neural crest cell distribution is disrupted in *Tbx1* homozygous mutants (Vitelli et al., 2002a). To understand whether this phenotype depends upon loss of mesodermal *Tbx1* expression, we used RNA in situ hybridization with a neural crest marker, *Crabp1* on M-ko embryos. The results revealed abnormal distribution of this cell population. Specifically, we detected reduced labeling of the pre-otic stream directed to the 2nd pharyngeal arch, apparent interruption of the post-otic stream directed to the 3rd pharyngeal arch and abnormal distribution of the circumpharyngeal stream (Fig. 2H,H′). Consistent with these data, we observed abnormalities of cranial nerve pathways (Fig. 2I,I′). Cranial nerves are partially derived from neural crest cells and have a similar migratory pathway. In M-ko embryos, the mandibular branch of the trigeminal (V) was fused caudally with the facial (VII) nerve. The glossopharyngeal (IX) nerve appeared hypoplastic. Terminal projections of the glossopharyngeal, the vagus (X) and the accessory (XI) showed disarray and were fused with each other (Fig. 2I,I′). These findings were similar to those observed in *Tbx1*-null mutants (Vitelli et al., 2002a). These results indicate that mesodermal *Tbx1* expression affects neural crest cell distribution.

Generation of a Cre-activatable *Tbx1* allele

Tissue-specific deletion can determine if an expression domain is necessary, but not if it is sufficient, for a particular developmental process. As *Tbx1* is expressed in multiple interacting tissues during pharyngeal development, it is reasonable to hypothesize that the gene may be necessary in multiple tissues to contribute to the complex morphogenesis of pharyngeal derivatives. To address this hypothesis, we designed and generated a new allele of *Tbx1* that has a low expression level but that can be reverted to wild-type level upon Cre recombination. To this end, we inserted a loxP-flanked PGKneo cassette into intron 5 by homologous recombination (Fig. 3A) and established the allele (*Tbx1*^{neo2}) in mice. We used quantitative real-time PCR to evaluate the amount of *Tbx1* mRNA in *Tbx1*$^{neo2/-}$ embryos at E9.5 and estimated that the allele produced ~20% of the wild-type mRNA level (data not shown). To establish whether there may be tissue-specific differences in *Tbx1* mRNA or protein expression, we used RNA in situ hybridization (not shown) and immunofluorescence on frozen section (Fig. 3B). With both techniques, we observed homogeneous, strong reduction of the signal without any obvious tissue differences. We predicted that removal of the PGKneo cassette by Cre recombination (generating the allele *Tbx1*$^{neo2\Delta}$) would revert this allele to a functionally 'normal' allele. Indeed, *Tbx1*$^{neo2\Delta/neo2\Delta}$ animals where viable, apparently normal and fertile (not shown). By contrast, *Tbx1*$^{neo2/+}$ and *Tbx1*$^{neo2/\Delta E5}$ animals presented with abnormalities similar to those observed in *Tbx1*$^{\Delta E5/+}$ and *Tbx1*$^{\Delta E5/\Delta E5}$ animals, respectively, as detailed below. To test whether the *neo2* allele could be reactivated in a tissue-specific manner, we crossed *Mesp1*$^{Cre/+}$;*Tbx1*$^{\Delta E5/+}$ with *Tbx1*$^{neo2/+}$ animals and carried out immunofluorescence on *Tbx1*$^{neo2/\Delta E5}$ and *Mesp1*$^{Cre/+}$;*Tbx1*$^{neo2/\Delta E5}$ E9.5 embryos, using an anti Tbx1 antibody on frozen sections. Results showed that although *Tbx1*$^{neo2/\Delta E5}$ embryos had near-background signal levels, *Mesp1*$^{Cre/+}$;*Tbx1*$^{neo2/\Delta E5}$ embryos had a robust signal in mesodermal tissues (Fig. 3B,B′). Thus, *Tbx1*^{neo2} is a hypomorphic allele that reverts to a functional allele upon Cre recombination in vivo. Because *Mesp1*^{Cre}-induced recombination precedes the onset of Tbx1 expression, it is predictable that the reactivation of the allele occurs from the onset of *Tbx1* expression.

Reactivation of mesodermal expression of *Tbx1* in a mutant background is sufficient to rescue most but not all the abnormalities of M-ko mutants

Tbx1$^{neo2/\Delta E5}$ embryos exhibited phenotypic abnormalities of the same type as those seen in *Tbx1*$^{\Delta E5/\Delta E5}$ embryos, although in some cases with a milder expressivity. Specifically, the cardiovascular

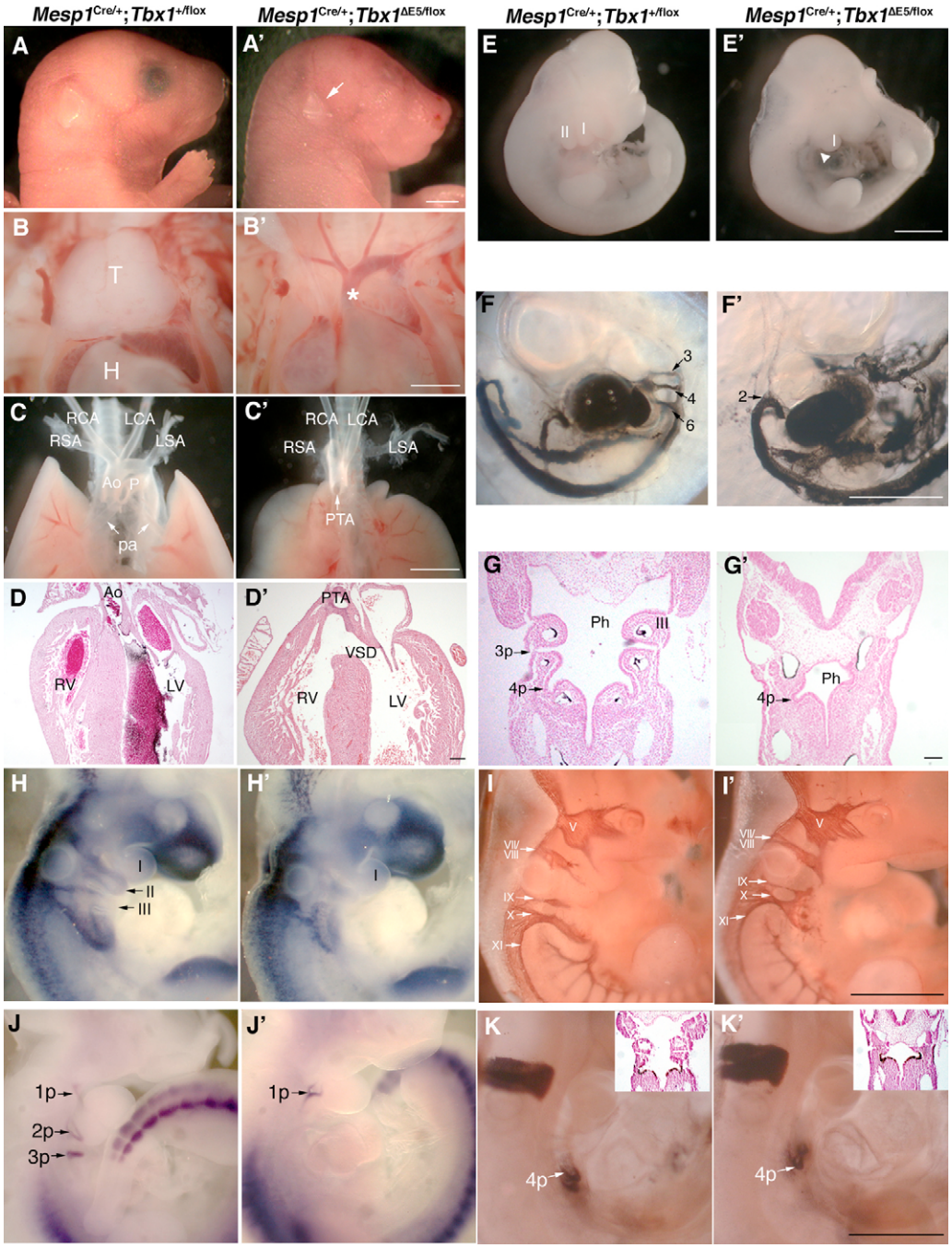

Fig. 2. Mesodermal ablation of *Tbx1* causes severe pharyngeal and cardiovascular abnormalities. (A-K) *Mesp1*$^{Cre/+}$;*Tbx1*$^{+/flox}$ control embryos compared with (A′-K′) *Mesp1*$^{Cre/+}$;*Tbx*$^{\Delta E5/flox}$ M-ko mutant embryos. Hypoplastic external ears (arrow **A**,**A′**), absence of thymus (T and asterisk, **B**,**B′**), persistent truncus arteriosus (PTA, **C**,**C′**) originating from the right ventricle (**D**,**D′**) and ventricular septal defect (VSD, D,D′) in M-ko embryos at E18.5. (**E**,**E′**) Hypoplasia of the 2nd pharyngeal arch (arrowhead) in an E10.5 M-ko embryo. (**F**,**F′**) Cardiac ink injection in E10.5 embryos visualized the 3rd, 4th and 6th pharyngeal arch arteries in cotrols (F); M-ko embryos have only one pair of arteries connecting the aortic sac with the dorsal aorta (F′). (**G**,**G′**) Coronal sections of E10.5 embryos revealed severe hypoplasia of the pharynx (Ph) in M-ko mutants. (**H**,**H′**) Whole-mount RNA in situ hybridization on E10 embryos using a *Crabp1* probe as a neural crest marker. Conditional deletion mutants showed abnormal *Crabp1* expressing pattern. (**I**,**I′**) Whole-mount immunohistochemistry on E10 embryos with an anti-neurofilament M antibody revealed abnormalities of cranial nerve pathways in the mutant. (**J**,**J′**) Whole-mount RNA in situ hybridization on E10 embryos with a *Pax1* probe revealed a small 1st pouch and loss of labeling of pouches 2 and 3 in M-ko mutants. (**K**,**K′**) Whole-mount immunohistochemistry on E10 embryos with an anti-Hoxb1 antibody revealed a normally specified, albeit slightly smaller, 4th pouch in M-ko mutants. The insets show coronal sections of the same embryos; the 4th pouches of M-ko embryos are not fully developed and not as close to the surface ectoderm as those of control embryos. T, thymus; H, heart; Ph, pharynx; Ao, aorta; P, pulmonary trunk; Pa, pulmonary artery; VSD, ventricular septum defect; RV/LV, right/left ventricle; RSA/LSA, right/left subclavian artery; RCA/LCA, right/left carotid artery; I, II and III, 1st, 2nd and 3rd pharyngeal arch; 3, 4 and 6, 3rd, 4th and 6th pharyngeal arch artery; 1p, 2p, 3p and 4p, 1st, 2nd, 3rd and 4th pharyngeal pouches; V, trigeminal nerve; VII/VIII, facial/acoustic nerve; IX, glossopharyngeal nerve; X, vagus nerve; XI, accessory nerve. Scale bars: 2 mm in A′; 1 mm in B′,C′,E′,F′,I′,K′; 100 μm in D′ and G′.

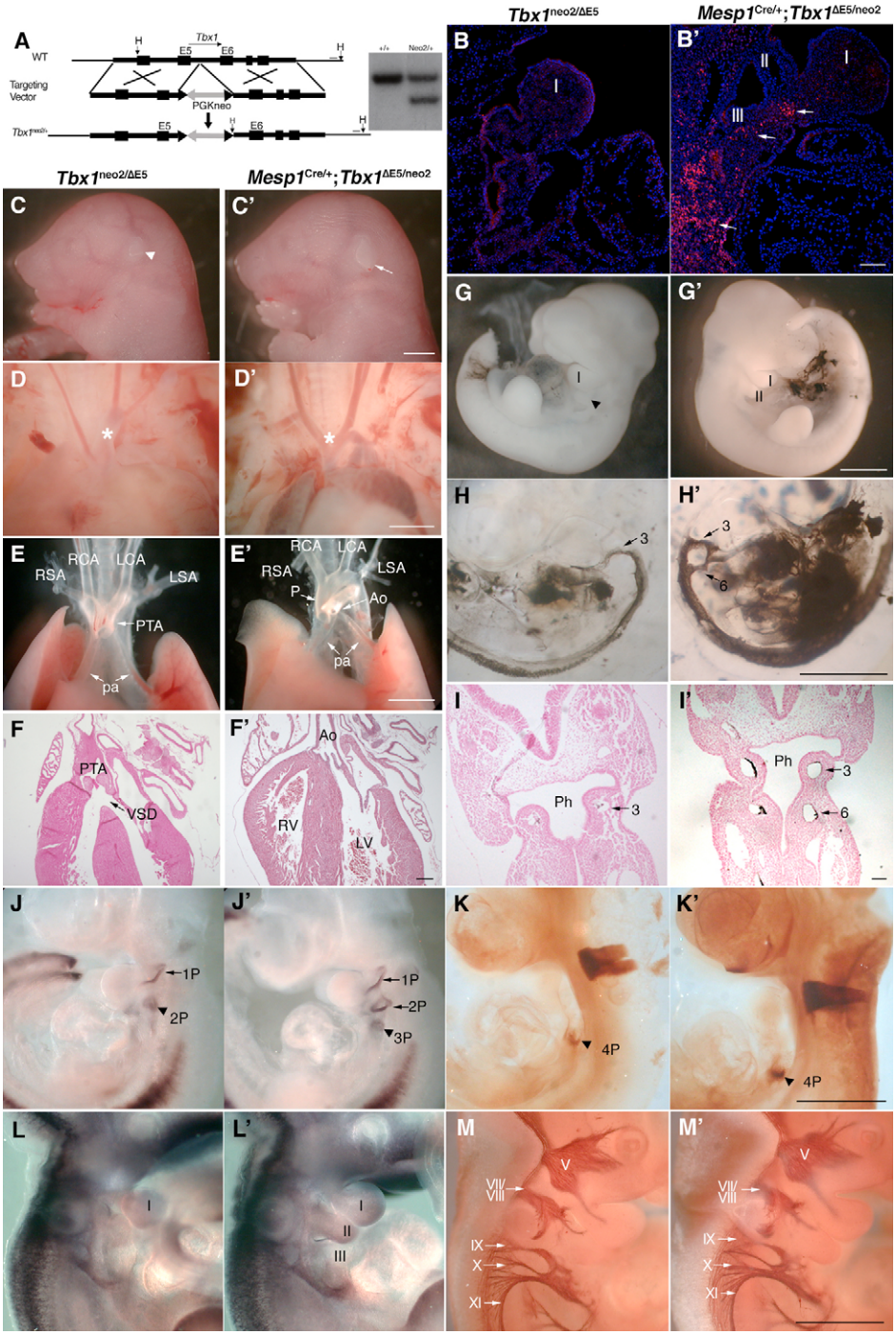

Fig. 3. Phenotypic analysis of compound mutants *Tbx1*$^{neo2/-}$ and conditional rescue mutants *Mesp1*$^{Cre/+}$;*Tbx1*$^{\Delta E5/neo2}$. (**A**) Scheme of gene targeting strategy. H, *Hin*dIII. (B-M) Compound mutants *Tbx1*$^{neo2/-}$. (B′-M′) Conditional rescue mutants *Mesp1*$^{Cre/+}$;*Tbx1*$^{\Delta E5/neo2}$. (**B**,**B′**) Immunohistochemistry using an anti-Tbx1 antibody on sagittal sections of E9.5 embryos showed very low or undetectable signal in compound mutants (B) and reactivated expression in the mesoderm (arrows) of the rescued embryo (B′). (**C**,**C′**) External ears (arrowhead) are hypoplastic in compound mutants but are of normal size in rescued mutants (arrow) at E18.5. (**D**,**D′**) Absence of thymus indicated by asterisk in both compound and rescued mutants at E18.5. (**E**,**E′**,**F**,**F′**) The cardiac outflow tract phenotype was normal in rescued embryos at E18.5. (**G**,**G′**) The hypoplasia of the 2nd pharyngeal arch of compound mutants (arrowhead) was corrected in rescued embryos. (**H**,**H′**) Ink injection into the heart of E10.5 embryos revealed normalization of the 6th pharyngeal arch arteries but not of the 4th pharyngeal arch arteries in rescued mutants. This is also evident from histological sections (**I**,**I′**). (**J**,**J′**) Whole-mount RNA in situ hybridization on E10 embryos with a *Paxl* probe revealed normalization of the 2nd pharyngeal pouch but only partial development of the 3rd pharyngeal pouch (arrowhead in J′) in rescued embryos. (**K**,**K′**) Whole-mount immunohistochemistry on E10 embryos with an anti-Hoxb1 antibody showed a more robust labeling of the 4th pouch (arrowhead) in rescued embryos. (**L**,**L′**) Whole-mount RNA in situ hybridization on E10 embryos with a *Crabp1* probe revealed only a marginal improvement of neural crest cell distribution in rescued embryos (compare with the normal pattern in Fig. 2H). Similarly, immunohistochemistry on E10 embryos using an anti neurofilament M antibody showed only modest improvement in rescued embryos, especially in the caudal region of the pharynx (**M**,**M′**), compare with normal pattern in Fig. 2I). Ph, pharynx; Ao, aorta; P, pulmonary trunk; Pa, pulmonary artery; VSD, ventricular septum defect; RV/LV, right/left ventricle; RSA/LSA, right/left subclavian artery; RCA/LCA, right/left carotid artery; I and II, 1st and 2nd pharyngeal arch; 3 and 6: 3rd and 6th pharyngeal arch artery; 1p, 2p, 3p and 4p, 1st, 2nd, 3rd and 4th pharyngeal pouches; V, trigeminal nerve; VII/VIII, facial/acoustic nerve; IX, glossopharyngeal nerve; X, vagus nerve; XI, accessory nerve. Scale bars: 2mm in C′; 1 mm in D′,E′,G′,H′,K′,M′; 100 μm in B′,F′,I′.

phenotype was very severe (n=20) and included PTA, aortic arch defects (Fig. 3E) and VSD (Fig. 3F). No thymus (n=17) could be observed except for three embryos that exhibited severe hypoplasia (Fig. 3D). The external ear (n=20) and the second pharyngeal arch (n=23) were hypoplastic (Fig. 3C,G). The latter two phenotypic abnormalities were present with different levels of severity but were never absent. The pharynx was hypoplastic and the 3rd, 4th, and 6th pharyngeal arches were not segmented (Fig. 3I). The 4th PAAs were absent in all the mutants (n=23), and the 3rd and/or 6th PAA were missing in one or both sides (Fig. 3H). Reactivation of mesodermal expression of *Tbx1* in *Mesp1*$^{Cre/+}$;*Tbx1*$^{neo2/\Delta E5}$ embryos rescued completely the OFT defects (PTA and VSD, Fig. 3E′,F′), the formation and remodeling of the 3rd and 6th pharyngeal arch arteries (Fig. 3H′,I′), and the hypoplasia of the 2nd pharyngeal arch and of

the external ear (Fig. 3C′,G′), but it did not rescue the thymic aplasia (Fig. 3D′) or the 4th pharyngeal arch and 4th PAA aplasia (Fig. 3H′,I′). The pharyngeal patterning defects were partially rescued. *Tbx1*$^{neo2/\Delta E5}$ embryos had a hypoplastic 2nd pharyngeal pouch and no detectable 3rd pouch, as detected by *Pax1* expression (Fig. 3J). Mesodermal reactivation was associated with normalized 2nd pouch signal and partial 3rd pouch signal (Fig. 3J′, compare with Fig. 2J for wild-type pattern). The 4th pharyngeal pouch (as revealed by Hoxb1 immunohistochemistry), was very hypoplastic in *Tbx1*$^{neo2/\Delta E5}$ embryos but was partially rescued by mesodermal reactivation of *Tbx1* (Fig. 3K,K′). Finally, the neural crest migration and cranial nerve pathway abnormalities observed in *Tbx1*$^{neo2/\Delta E5}$ embryos were only marginally improved by mesodermal reactivation (Fig. 3L,L′,M,M′, compare with Fig. 2H,I for wild-type patterns).

Overall, these rescue experiments identified processes that are exquisitely dependent upon mesodermal expression of *Tbx1*. These are OFT development, 2nd pharyngeal arch morphogenesis, 3rd and 6th pharyngeal arch arteries. By contrast, 4th pharyngeal arch and PAA morphogenesis, thymic development, neural crest migration and cranial nerve guidance are dependent upon expression in the mesoderm and epithelia.

Mesodermal expression of *Tbx1* is required to maintain proliferation and *Fgf8* expression cell autonomously

Having defined the mesoderm-specific developmental roles of Tbx1, we asked how these roles may be effected. Timed deletion of *Tbx1* has shown that the structures affected by mesodermal-specific gene ablation require *Tbx1* approximately between E8.0 and E9.0 (Xu et al., 2005). We, therefore, focused our attention on E8.5 M-ko embryos. The *Tbx1* gene is turned on at approximately E8 in the paraxial mesoderm, and in the adjacent ectoderm and endoderm (Fig. 4A,A′). At these stages, M-ko mutants were indistinguishable from controls. However, immunostaining with anti-phospho H3 antibody, which detects mitotic cells, showed that mutants had severely reduced mitotic activity (Fig. 4B,B′,E). By contrast, immunostaining with an anti-cleaved caspase 3 antibody did not reveal changes in apoptotic activity (data not shown). It has been shown that *Tbx1* interacts with and may directly regulate *Fgf8* gene expression (Hu et al., 2004; Vitelli et al., 2002b), and loss of *Fgf8* can downregulate mitotic activity in pharyngeal mesoderm (Park et al., 2006). Therefore, we tested *Fgf8* expression in M-ko mutants at E8.5, E9.0 and E9.5. At all stages tested, the pharyngeal epithelial expression of *Fgf8* was conserved (with the caveat that the pharynx of M-ko embryos is hypoplastic, and, therefore, expression domains appear proportionally smaller) (Fig. 5). By contrast, the early splanchnic mesoderm/anterior heart field domain detectable at E8.5, was lost or strongly downregulated (Fig. 5A′-B′). This region also expresses *Tbx1* (Nowotschin et al., 2006; Zhang et al., 2005). *Shh* expression was maintained at all the stages tested (E8.5, E9.0 and E9.5, not shown). Thus, reduced proliferation of mesenchymal cells in M-ko embryos may be secondary to downregulation of autocrine Fgf8 signaling, but it is unlikely to be secondary to loss of epithelial signals.

DISCUSSION

The pharyngeal mesoderm plays a crucial role in pharyngeal patterning

The function of pharyngeal mesoderm in craniofacial myogenesis has been extensively investigated (Hacker and Guthrie, 1998; Kelly et al., 2004; Noden and Francis-West, 2006), but little is known

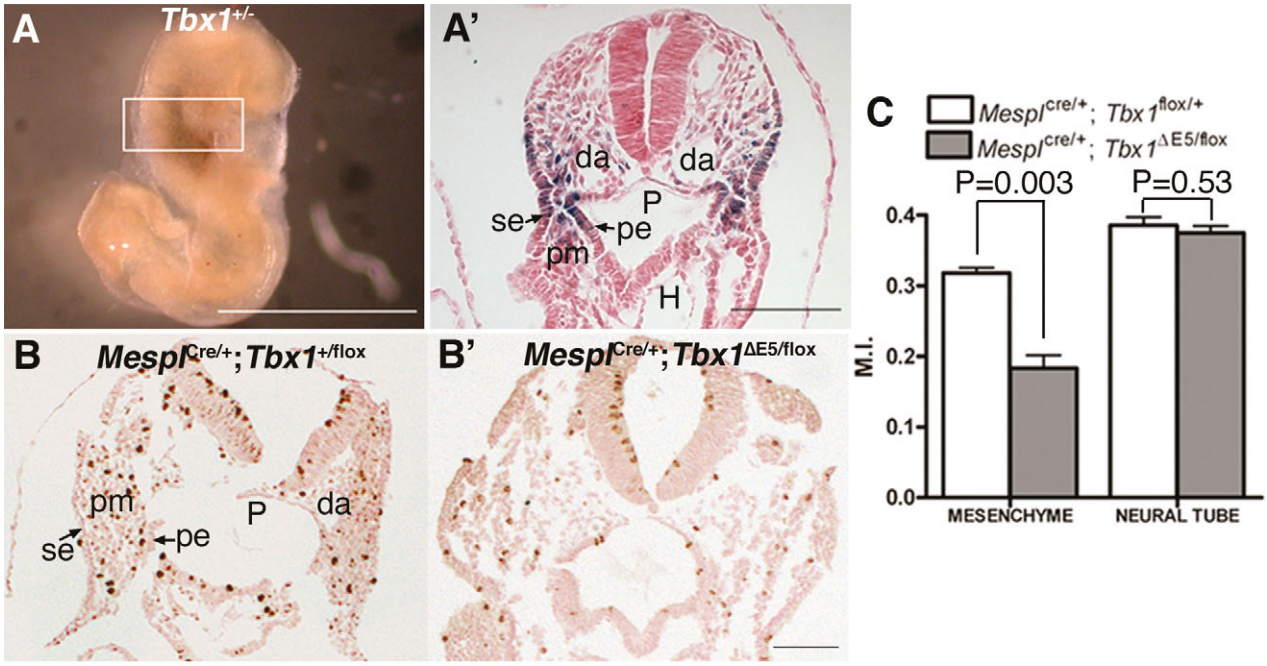

Fig. 4. *Tbx1* regulates cell proliferation in mesenchyme cells. (**A**,**A′**) *Tbx1* expression domain revealed by a *Tbx1*-lacZ knock-in allele (*Tbx1*$^{+/-}$) at E8.5. (A′) Transverse section of A. The area where cell proliferation was scored is indicated by the white box in A. (**B**) Transverse sections of E8.5 *Mesp1*$^{Cre/+}$; *Tbx1*$^{+/flox}$ embryos as controls. (**B′**) Transverse sections of E8.5 *Mesp1*$^{Cre/+}$; *Tbx1*$^{\Delta E5/flox}$ embryos. (B,B′) Immunohistochemistry staining with an anti-phospho-Histone H3 antibody to evaluate cell proliferation. (**C**) Mitotic index (M.I.) in pharyngeal mesenchyme at E8.5 embryos. Cells in neural tube were counted as an internal control. *P* values were calculated using Student's *t*-test. da, dorsal aorta; se, surface ectoderm; pe, pharyngeal ectoderm; pm, pharyngeal mesenchyme; P, pharynx. Scale bars: 1 mm in A; 100 μm in A′-B′.

about its role in pharyngeal segmentation. Here, we show that loss of *Tbx1* expression in the mesoderm suppresses pharyngeal pouch and posterior pharyngeal arch formation, and disrupts the distribution of neural crest-derived cells. These observations support a crucial role of the mesoderm in pharyngeal segmentation.

The pharyngeal mesoderm is composed of cells migrating from the cranial paraxial mesoderm (Trainor and Tam, 1995; Trainor et al., 1994), which is loosely packed into meristic cell clusters called somitomeres (Tam and Trainor, 1994). The somitomeristic mesoderm underlying the neural tube has a topographic relation to specific neural tube segments, and has regionalized cell fate along the craniocaudal axis. Cells migrate and colonize specific pharyngeal arches along with cranial neural crest cells from the same axial level (Trainor and Tam, 1995). Unlike the cranial neural crest streams, which are characterized by discrete *Hox* gene expression profiles (Hunt et al., 1991a; Hunt et al., 1991b), individual somitomeres do not appear to be identifiable by a gene expression code. Pharyngeal mesoderm was shown to provide permissive signals to maintain the identity of neural crest cell populations (Trainor and Krumlauf, 2000), and to generate 'exclusion zones' separating streams of neural crest cells (Trainor et al., 2002b). However, it is unlikely that this function of the mesoderm is essential for pharyngeal segmentation, because neural crest cell ablation is not sufficient to disrupt pharyngeal segmentation (Veitch et al., 1999). Mesodermal *Tbx1* is necessary but not sufficient for normal neural crest migration, whereas it is necessary and sufficient for, at least part of, the segmentation process. This suggests that the role of the mesoderm in segmentation may be cell-autonomous and/or dependent upon mesoderm-epithelial interactions. This is consistent with the findings that wild-type mesoderm can partially rescue pharyngeal segmentation defects in *fgf8*$^{-}$;*fgf3*-MO zebrafish mutants (Crump et al., 2004).

Mesodermal *Tbx1* is necessary and sufficient for cardiac outflow tract development

We have previously proposed that *Tbx1* has a role in the expansion of cardiomyocyte precursors, but we were not able to exclude that at least part of the cardiac outflow tract phenotype may be due to reduced endodermal expression (Xu et al., 2005; Xu et al., 2004). This is because the key Cre driver used in those experiments, *Nkx2.5*^{Cre}, induced recombination in a region of the pharyngeal endoderm partially overlapping with *Tbx1* expression (Xu et al., 2004). Here, we show that mesodermal ablation recapitulated the OFT abnormalities seen in *Tbx1*$^{-/-}$ embryos, whereas mesodermal *Tbx1* restoration in a mutant background was sufficient to rescue those abnormalities. These results suggest that the role of endoderm expression in cardiac outflow development is marginal, if at all important, and assign the crucial role to mesodermal expression. However, Arnold et al. (Arnold et al., 2006) have shown that *Tbx1* ablation using the *Foxg1*$^{Cre/+}$ driver results in a severe phenotype (including OFT defects) resembling that of *Tbx1*$^{-/-}$ animals. The report showed that this driver induced recombination predominantly in the pharyngeal endoderm, suggesting a major role of *Tbx1* in this tissue for OFT development. We have shown that the *Foxg1*$^{Cre/+}$ driver induces robust recombination not only in pharyngeal epithelia (endoderm and ectoderm) but also in pharyngeal mesoderm and secondary heart field (Zhang et al., 2005). Arnold et al. have used this driver in a different genetic background that clearly has attenuated extra-endodermal recombination. However, it cannot be excluded that residual recombination activity in the mesoderm might have reduced the dose of Tbx1 in this tissue to a level that affects normal OFT development.

Tissue-specific roles of *Tbx1*: not always a clear cut distinction

Ablation of a gene from individual interacting tissues may potentially lead to similar morphological phenotypes without necessarily illuminating the role of the gene in a particular tissue. The strategy used here, i.e. tissue-specific gene reactivation in a mutant background, was designed to diminish this problem. *Mesp1*^{Cre}-driven deletion and restoration of *Tbx1* expression showed that Tbx1 has several developmental roles that are confined to the mesoderm. However, the development of the thymus, of the 3rd and 4th pharyngeal pouches, and of the 4th pharyngeal arch require both mesodermal and epithelial

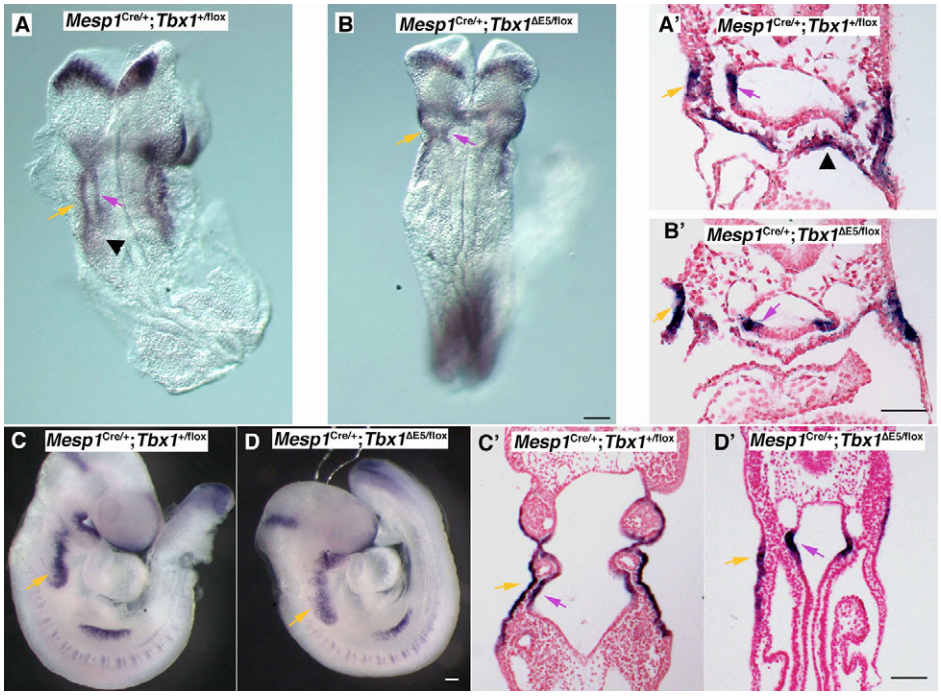

Fig. 5. Mesodermal *Tbx1* affects mesodermal but not epithelial *Fgf8* expression. (**A-D**) Whole-mount RNA in situ hybridization with an *Fgf8* probe. (**A′**,**B′**) Transverse sections of the E8.5 embryos shown in A and B, respectively. (**C′**,**D′**) Coronal sections of the E9 embryos shown in C and D, respectively. Orange arrows indicate *Fgf8* expression in the ectoderm. Pink arrows indicate *Fgf8* expression in endoderm. Black arrowheads indicate *Fgf8* expression in splanchnic mesoderm/anterior heart field. Scale bar: 100 μm in B,D,D′; 50 μm in B′.

expression. Thus, besides a cell-autonomous function in the mesoderm, Tbx1 may regulate interactions between different tissues. Exactly how this role is effected remains to be clarified, but considering that *Tbx1* appears to interact with several of the major signaling systems that play fundamental roles in development, the candidate molecular pathways are manifold. Mechanisms could include transcriptional regulation of genes encoding extracellular ligands (Hu et al., 2004; Vitelli et al., 2002b; Xu et al., 2004) or of proteins involved in the catabolism of ligands (Guris et al., 2006; Ivins et al., 2005) or in signal transduction (Park et al., 2006).

The fact that the $Tbx1^{Neo2}$ allele is not null raises the issue of whether the rescue of some phenotypic abnormalities in the restoration experiments might have been 'helped' by the residual expression of the *neo2* allele in the endoderm and ectoderm. However, the observations that $Tbx1^{neo2/-}$ embryos have essentially the same phenotype as $Tbx1^{-/-}$ embryos and that $Mesp1^{Cre/+};Tbx1^{floxl-}$ animals also have a very severe and similar phenotype to $Tbx1^{-/-}$ embryos, suggest that reduced or full expression of *Tbx1* in non-mesodermal tissues, although required for several developmental processes, cannot rescue phenotypic abnormalities caused by loss of mesodermal *Tbx1* expression.

What is the role of *Tbx1* in the mesoderm?

To understand the earliest molecular consequences of *Tbx1* loss of function in the mesoderm, we examined M-ko mutants at a stage previously shown to be crucial for *Tbx1* function. At this stage (E8.5), the morphology of mutant embryos is normal but we found a strong reduction in cell proliferation in the region of the pharyngeal mesenchyme that normally expresses *Tbx1*. Such reduced proliferation could explain the strongly reduced cellularity in the pharyngeal arches and the cardiac outflow tract defects. Ataliotis et al. using lineage labeling experiments in *Xenopus*, suggested that *Tbx1* has a cell-autonomous function in the pharyngeal mesoderm (Ataliotis et al., 2005).

We and others have proposed that the Tbx1 pro-proliferative activity may be effected, at least in part, by regulating FGF ligand gene expression. This view is supported by the demonstration that Tbx1 can indeed activate an *Fgf8* enhancer in tissue culture assays (Hu et al., 2004), and by the genetic interaction between the two genes in vivo (Vitelli et al., 2002b; Vitelli et al., 2006). It has been shown that conditional ablation of *Fgf8* in the mesoderm can cause OFT defects and reduce cell proliferation and survival (Ilagan et al., 2006; Park et al., 2006). We and others have previously shown that *Tbx1* is required for endodermal, but not ectodermal, expression (Zhang et al., 2005), but *Fgf8* expression in the mesoderm of *Tbx1* mutants had not been tested before. Here, we show that mesodermal *Tbx1* is required for *Fgf8* expression in the splanchnic mesoderm/anterior heart field region. Whether or not the loss of *Fgf8* in this tissue is sufficient to cause the OFT phenotype of M-ko mutants is unknown. $Mesp1^{Cre}$-driven deletion of *Fgf8* causes early lethality in most embryos, preventing the full assessment of fetal consequences of this conditional mutation (Park et al., 2006). However, *Fgf8* knock-in into the *Tbx1* locus was unable to rescue or modify the OFT phenotype of *Tbx1* mutants (Vitelli et al., 2006). In addition, *Fgf8* loss in mesoderm reduces cell survival and proliferation, while *Tbx1* mutation only affects proliferation. Further complication of the relationship between *Tbx1* and *Fgf8*, is added by the report of downregulation of the FGF receptor *Fgfr1* RNA expression in $Tbx1^{-/-}$ mutants (Park et al., 2006). We propose that a reduction of FGF signaling, resulting from cell autonomous downregulation of ligand and receptor expression, has an important role in the cell proliferation phenotype of *Tbx1* mutants. However, the role of other signaling systems should be investigated.

Overall, our data indicate a crucial role of the mesoderm in the pathogenesis of the DiGeorge-like phenotype and we show, for the first time, that the mesoderm has a direct influence on the proper morphogenesis of the pharyngeal pouches.

We thank A. Sobotka, G. Ji, P. Terrell, M. Woods and W. Yu for invaluable technical assistance; Y. Saga for $Mesp1^{Cre}$ mice and N. Manley for anti-Hoxb1 antibody; and E. Lindsay and J. Martin for critical reading of the manuscript. This work was funded by grants HL051524, HL064832 and HL067155 from the National Institutes of Health (to A.B.).

References

Albrecht, U., Eichele, G., Helms, J. A. and Lu, H. C. (1997). Visualization of gene expression patterns by in situ hybridization. In *Molecular and Cellular Methods in Developmental Toxicology* (ed. G. P. Daston), pp. 23-48. New York: CRC Press.

Arnold, J. S., Werling, U., Braunstein, E. M., Liao, J., Nowotschin, S., Edelmann, W., Hebert, J. M. and Morrow, B. E. (2006). Inactivation of Tbx1 in the pharyngeal endoderm results in 22q11DS malformations. *Development* **133**, 977-987.

Ataliotis, P., Ivins, S., Mohun, T. J. and Scambler, P. J. (2005). XTbx1 is a transcriptional activator involved in head and pharyngeal arch development in Xenopus laevis. *Dev. Dyn.* **232**, 979-991.

Chapman, D. L., Garvey, N., Hancock, S., Alexiou, M., Agulnik, S. I., Gibson-Brown, J. J., Cebra-Thomas, J., Bollag, R. J., Silver, L. M. and Papaioannou, V. E. (1996). Expression of the T-box family genes, Tbx1-Tbx5, during early mouse development. *Dev. Dyn.* **206**, 379-390.

Chen, A., Francis, M., Ni, L., Cremers, C. W., Kimberling, W. J., Sato, Y., Phelps, P. D., Bellman, S. C., Wagner, M. J., Pembrey, M. et al. (1995). Phenotypic manifestations of branchio-oto-renal syndrome. *Am. J. Med. Genet.* **58**, 365-370.

Crump, J. G., Maves, L., Lawson, N. D., Weinstein, B. M. and Kimmel, C. B. (2004). An essential role for Fgfs in endodermal pouch formation influences later craniofacial skeletal patterning. *Development* **131**, 5703-5716.

Giguere, V., Lyn, S., Yip, P., Siu, C. H. and Amin, S. (1990). Molecular cloning of cDNA encoding a second cellular retinoic acid- binding protein. *Proc. Natl. Acad. Sci. USA* **87**, 6233-6237.

Graham, A., Okabe, M. and Quinlan, R. (2005). The role of the endoderm in the development and evolution of the pharyngeal arches. *J. Anat.* **207**, 479-487.

Guris, D. L., Duester, G., Papaioannou, V. E. and Imamoto, A. (2006). Dose-dependent interaction of Tbx1 and Crkl and locally aberrant RA signaling in a model of del22q11 syndrome. *Dev. Cell* **10**, 81-92.

Hacker, A. and Guthrie, S. (1998). A distinct developmental programme for the cranial paraxial mesoderm in the chick embryo. *Development* **125**, 3461-3472.

Helms, J. A. and Schneider, R. A. (2003). Cranial skeletal biology. *Nature* **423**, 326-331.

Hu, T., Yamagishi, H., Maeda, J., McAnally, J., Yamagishi, C. and Srivastava, D. (2004). Tbx1 regulates fibroblast growth factors in the anterior heart field through a reinforcing autoregulatory loop involving forkhead transcription factors. *Development* **131**, 5491-5502.

Hunt, P., Gulisano, M., Cook, M., Sham, M. H., Faiella, A., Wilkinson, D., Boncinelli, E. and Krumlauf, R. (1991a). A distinct Hox code for the branchial region of the vertebrate head. *Nature* **353**, 861-864.

Hunt, P., Whiting, J., Muchamore, I., Marshall, H. and Krumlauf, R. (1991b). Homeobox genes and models for patterning the hindbrain and branchial arches. *Dev. Suppl.* **1**, 187-196.

Ilagan, R., Abu-Issa, R., Brown, D., Yang, Y. P., Jiao, K., Schwartz, R. J., Klingensmith, J. and Meyers, E. N. (2006). Fgf8 is required for anterior heart field development. *Development* **133**, 2435-2445.

Ivins, S., Lammerts van Beuren, K., Roberts, C., James, C., Lindsay, E., Baldini, A., Ataliotis, P. and Scambler, P. J. (2005). Microarray analysis detects differentially expressed genes in the pharyngeal region of mice lacking Tbx1. *Dev. Biol.* **285**, 554-569.

Jerome, L. A. and Papaioannou, V. E. (2001). DiGeorge syndrome phenotype in mice mutant for the T-box gene, *Tbx1*. *Nat. Genet.* **27**, 286-291.

Kelly, R. G., Jerome-Majewska, L. A. and Papaioannou, V. E. (2004). The del22q11.2 candidate gene Tbx1 regulates branchiomeric myogenesis. *Hum. Mol. Genet.* **13**, 2829-2840.

Liao, J., Kochilas, L., Nowotschin, S., Arnold, J. S., Aggarwal, V. S., Epstein, J. A., Brown, M. C., Adams, J. and Morrow, B. E. (2004). Full spectrum of malformations in velo-cardio-facial syndrome/DiGeorge syndrome mouse models by altering Tbx1 dosage. *Hum. Mol. Genet.* **13**, 1577-1585.

Lindsay, E. A. (2001). Chromosomal microdeletions: dissecting del22q11 syndrome. *Nat. Rev. Genet.* **2**, 858-868.

Lindsay, E. A., Vitelli, F., Su, H., Morishima, M., Huynh, T., Pramparo, T., Jurecic, V., Ogunrinu, G., Sutherland, H. F., Scambler, P. J. et al. (2001).

Tbx1 haploinsufficieny in the DiGeorge syndrome region causes aortic arch defects in mice. *Nature* **410**, 97-101.
Merscher, S., Funke, B., Epstein, J. A., Heyer, J., Puech, A., Lu, M. M., Xavier, R. J., Demay, M. B., Russell, R. G., Factor, S. et al. (2001). TBX1 is responsible for cardiovascular defects in Velo-Cardio-Facial/DiGeorge Syndrome. *Cell* **104**, 619-629.
Noden, D. M. (1983). The role of the neural crest in patterning of avian cranial skeletal, connective, and muscle tissues. *Dev. Biol.* **96**, 144-165.
Noden, D. M. and Francis-West, P. (2006). The differentiation and morphogenesis of craniofacial muscles. *Dev. Dyn*. **235**, 1194-1218.
Nowotschin, S., Liao, J., Gage, P. J., Epstein, J. A., Campione, M. and Morrow, B. E. (2006). Tbx1 affects asymmetric cardiac morphogenesis by regulating Pitx2 in the secondary heart field. *Development* **133**, 1565-1573.
Park, E. J., Ogden, L. A., Talbot, A., Evans, S., Cai, C. L., Black, B. L., Frank, D. U. and Moon, A. M. (2006). Required, tissue-specific roles for Fgf8 in outflow tract formation and remodeling. *Development* **133**, 2419-2433.
Piotrowski, T. and Nusslein-Volhard, C. (2000). The endoderm plays an important role in patterning the segmented pharyngeal region in zebrafish (Danio rerio). *Dev. Biol.* **225**, 339-356.
Piotrowski, T., Ahn, D. G., Schilling, T. F., Nair, S., Ruvinsky, I., Geisler, R., Rauch, G. J., Haffter, P., Zon, L. I., Zhou, Y. et al. (2003). The zebrafish van gogh mutation disrupts tbx1, which is involved in the DiGeorge deletion syndrome in humans. *Development* **130**, 5043-5052.
Roberts, C., Ivins, S. M., James, C. T. and Scambler, P. J. (2005). Retinoic acid down-regulates Tbx1 expression in vivo and in vitro. *Dev. Dyn.* **232**, 928-938.
Robin, N. H., Feldman, G. J., Aronson, A. L., Mitchell, H. F., Weksberg, R., Leonard, C. O., Burton, B. K., Josephson, K. D., Laxova, R., Aleck, K. A. et al. (1995). Opitz syndrome is genetically heterogeneous, with one locus on Xp22, and a second locus on 22q11.2. *Nat. Genet.* **11**, 459-461.
Saga, Y., Miyagawa-Tomita, S., Takagi, A., Kitajima, S., Miyazaki, J. and Inoue, T. (1999). MesP1 is expressed in the heart precursor cells and required for the formation of a single heart tube. *Development* **126**, 3437-3447.
Saldivar, J. R., Krull, C. E., Krumlauf, R., Ariza-McNaughton, L. and Bronner-Fraser, M. (1996). Rhombomere of origin determines autonomous versus environmentally regulated expression of Hoxa-3 in the avian embryo. *Development* **122**, 895-904.
Schneider, R. A. and Helms, J. A. (2003). The cellular and molecular origins of beak morphology. *Science* **299**, 565-568.
Soriano, P. (1999). Generalized lacZ expression with the ROSA26 Cre reporter strain [letter]. *Nat. Genet.* **21**, 70-71.
Stalmans, I., Lambrechts, D., De Smet, F., Jansen, S., Wang, J., Maity, S., Kneer, P., Von Der Ohe, M., Swillen, A., Maes, C. et al. (2003). VEGF: A modifier of the del22q11 (DiGeorge) syndrome? *Nat. Med.* **9**, 173-182.
Tam, P. P. and Trainor, P. A. (1994). Specification and segmentation of the paraxial mesoderm. *Anat. Embryol.* **189**, 275-305.
Trainor, P. A. and Tam, P. P. (1995). Cranial paraxial mesoderm and neural crest cells of the mouse embryo: co-distribution in the craniofacial mesenchyme but distinct segregation in branchial arches. *Development* **121**, 2569-2582.
Trainor, P. and Krumlauf, R. (2000). Plasticity in mouse neural crest cells reveals a new patterning role for cranial mesoderm. *Nat. Cell Biol.* **2**, 96-102.
Trainor, P. A., Tan, S. S. and Tam, P. P. (1994). Cranial paraxial mesoderm: regionalisation of cell fate and impact on craniofacial development in mouse embryos. *Development* **120**, 2397-2408.
Trainor, P. A., Ariza-McNaughton, L. and Krumlauf, R. (2002a). Role of the isthmus and FGFs in resolving the paradox of neural crest plasticity and prepatterning. *Science* **295**, 1288-1291.
Trainor, P. A., Sobieszczuk, D., Wilkinson, D. and Krumlauf, R. (2002b). Signalling between the hindbrain and paraxial tissues dictates neural crest migration pathways. *Development* **129**, 433-442.
Veitch, E., Begbie, J., Schilling, T. F., Smith, M. M. and Graham, A. (1999). Pharyngeal arch patterning in the absence of neural crest. *Curr. Biol.* **9**, 1481-1484.
Vitelli, F., Morishima, M., Taddei, I., Lindsay, E. A. and Baldini, A. (2002a). Tbx1 mutation causes multiple cardiovascular defects and disrupts neural crest and cranial nerve migratory pathways. *Hum. Mol. Genet.* **11**, 915-922.
Vitelli, F., Taddei, I., Morishima, M., Meyers, E. N., Lindsay, E. A. and Baldini, A. (2002b). A genetic link between Tbx1 and Fibroblast Growth Factor signaling. *Development* **129**, 4605-4611.
Vitelli, F., Zhang, Z., Huynh, T., Sobotka, A., Mupo, A. and Baldini, A. (2006). Fgf8 expression in the Tbx1 domain causes skeletal abnormalities and modifies the aortic arch but not the outflow tract phenotype of Tbx1 mutants. *Dev. Biol.* **295**, 559-570.
Xu, H., Morishima, M., Wylie, J. N., Schwartz, R. J., Bruneau, B. G., Lindsay, E. A. and Baldini, A. (2004). Tbx1 has a dual role in the morphogenesis of the cardiac outflow tract. *Development* **131**, 3217-3227.
Xu, H., Cerrato, F. and Baldini, A. (2005). Timed mutation and cell-fate mapping reveal reiterated roles of Tbx1 during embryogenesis, and a crucial function during segmentation of the pharyngeal system via regulation of endoderm expansion. *Development* **132**, 4387-4395.
Yagi, H., Furutani, Y., Hamada, H., Sasaki, T., Asakawa, S., Minoshima, S., Ichida, F., Joo, K., Kimura, M., Imamura, S.-I. et al. (2003). Role of TBX1 in human del22q11.2 syndrome. *Lancet* **362**, 1366-1373.
Yamagishi, H., Maeda, J., Hu, T., McAnally, J., Conway, S. J., Kume, T., Meyers, E. N., Yamagishi, C. and Srivastava, D. (2003). Tbx1 is regulated by tissue-specific forkhead proteins through a common Sonic hedgehog-responsive enhancer. *Genes Dev.* **17**, 269-281.
Zhang, Z., Cerrato, F., Xu, H., Vitelli, F., Morishima, M., Vincentz, J., Furuta, Y., Ma, L., Martin, J. F., Baldini, A. et al. (2005). Tbx1 expression in pharyngeal epithelia is necessary for pharyngeal arch artery development. *Development* **132**, 5307-5315.